# Safety-Critical Connected Cruise Control: Leveraging Connectivity for Safe and Efficient Longitudinal Control of Automated Vehicles

Yuchen Chen, Gábor Orosz, and Tamas G. Molnar

***Abstract*— Leveraging connectivity for controlling connected automated vehicles (CAVs) has great potential for improving the safety and efficiency of transportation. In this paper, we study the safety of connected cruise control (CCC), wherein CAVs respond to multiple preceding vehicles via vehicle-to-everything (V2X) connectivity. Using control barrier function theory, we analyze how connectivity to vehicles farther ahead can be leveraged to improve the CAV's safety, and we propose *safety-critical CCC* by minimally modifying efficient but not always safe CCC designs. We use simulations to evaluate the proposed safety-critical CCC with respect to safety, energy efficiency and string stability. We also study mixed traffic, and show that increasing the penetration of CAVs can significantly improve safety and performance of road transportation systems.**

## I. INTRODUCTION

Vehicle-to-everything (V2X) communication offers benefits for the control of connected automated vehicles (CAVs) in terms of safety, fuel efficiency, and driving behavior. Using connectivity, CAVs can get information from and respond to other connected road participants, which may significantly improve their performance. For example, connectivity enables CAVs to exchange information with other connected vehicles ahead of them, and use this information in on-board controllers such as *connected cruise control (CCC)* [1]. Effectively designed CAV controllers have demonstrated a variety of benefits, including better fuel economy [2] and traffic congestion mitigation [3], [4].

A primary focus when deploying CAVs is safety. Recent works have focused on safety-critical control for CAVs. Existing approaches include reachability analysis [5], formal methods [6], and model predictive control [7]. Furthermore, control barrier functions (CBFs) have shown notable success in control synthesis because of their high adaptability to existing control frameworks. CBFs have been applied in adaptive cruise control [8], lane changing [9], traffic control by CAVs [10] and experiments [11]. Safe CCC was established by CBFs in [12], which was followed by a detailed analysis in [13] and experiments using a heavy-duty truck in [14]. However, these works only considered cases where the CAV responds to the immediate preceding vehicle, lacking investigation on the relationship between connectivity architecture and safety.

Y. Chen is with the Department of Mechanical Engineering, University of Michigan, Ann Arbor, MI 48109, USA, ethanch@umich.edu.

G. Orosz is with the Department of Mechanical Engineering and with the Department of Civil and Environmental Engineering, University of Michigan, Ann Arbor, MI 48109, USA, orosz@umich.edu.

T. G. Molnar is with the Department of Mechanical Engineering, Wichita State University, Wichita, KS 67260, USA, tamas.molnar@wichita.edu.

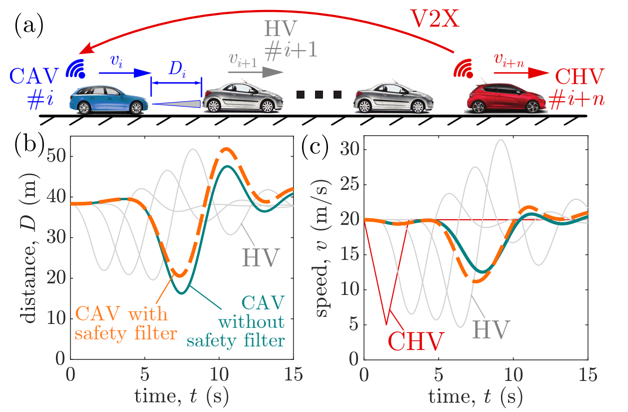


Fig. 1. (a) Connected cruise control (CCC) where a connected automated vehicle (CAV) responds to a human-driven vehicle (HV) and a connected human-driven vehicle (CHV). (b)-(c) Behavior of CCC with unsafe choice of controller parameters (teal), and the proposed safety-critical CCC that involves active interventions by a safety filter (orange).

In this paper, we analyze how connectivity between the CAV and vehicles farther ahead affects the safety of existing CCC laws and provide safe choices of CCC parameters. We show that tuning existing CCC laws to always maintain safety becomes more challenging or even impossible as the CAV connects to vehicles farther ahead, making it difficult to exploit the full potential of connectivity to improve performance. Meanwhile, existing high-performance CCC designs may not be safe in all scenarios. To remedy this trade-off, we propose *safety-critical CCC* that minimally modifies existing, efficient but potentially unsafe CCC designs to guarantee safety, see Fig. 1. By intervening only when there is danger, the proposed controller achieves the best of both worlds: safe behavior and high performance.

The rest of this paper is organized as follows. In Section II, we establish longitudinal car-following models and introduce CCC. In Section III, we first revisit the CBF theory, then we provide guideline for safe nominal CCC design and propose *safety-critical CCC*. In Section IV, we simulate the proposed controller in mixed traffic. Finally, we conclude our results and propose future directions in Section V.

## II. CONNECTED CRUISE CONTROL

Consider the scenario in Fig. 1(a), where a connected automated vehicle (CAV) follows a chain of human-driven vehicles (HVs) while responding to a connected human-driven vehicle (CHV) that is $n$ vehicles ahead. We assume that the CAV measures its own speed $v_i$, the preceding HV's speed $v_{i+1}$ and the distance $D_i$ via on-board range sensors, while it acquires the CHV's speed $v_{i+n}$ via vehicle-to-everything (V2X) connectivity.

We model the HVs' dynamics by:

$$\begin{aligned}\dot{D}_{i+j}(t) &= v_{i+j+1}(t) - v_{i+j}(t),\\ \dot{v}_{i+j}(t) &= u_{i+j}(t-\tau), \quad \forall j \in \{1,\ldots,n-1\},\end{aligned} \tag{1}$$

where the delay $\tau$ captures the driver reaction time and powertrain delays and the car-following behavior is modeled by the optimal velocity model (OVM) [15]:

$$u_{i+j} = A_{\rm h}\big(V_{\rm h}(D_{i+j}) - v_{i+j}\big) + B_{\rm h}\big(v_{i+j+1} - v_{i+j}\big). \tag{2}$$

That is, the HV responds to the speed difference using gain $B_{\rm h}$ and to the distance using gain $A_{\rm h}$ and the range policy:

$$V_{\rm h}(D) = \min\{\kappa_{\rm h}(D - D_{\rm st}), v_{\max}\}. \tag{3}$$

This range policy prescribes a desired speed as a function of the distance, which is zero at the standstill distance $D_{\rm st}$ and increases linearly up to speed limit $v_{\max}$ with gradient $\kappa_{\rm h}$.

We model the CAV's dynamics by:

$$\begin{aligned}\dot{D}_i(t) &= v_{i+1}(t) - v_i(t),\\ \dot{v}_i(t) &= u_i(t),\end{aligned} \tag{4}$$

and the CAV's state is denoted as $x = [D_i \ v_i]^\top$. To reduce the complexity of the control design, we neglect the input delays [16] and input constraints [17]. We choose the desired controller $u_i = k_{\rm d}(x)$, to be the *connected cruise control (CCC)* strategy given in [1] and experimentally tested in [18]:

$$\begin{aligned}k_{\rm d}(x) = A\big(V(D_i) - v_i\big) &+ B_1\big(W(v_{i+1}) - v_i\big)\\ &+ B_n\big(W(v_{i+n}) - v_i\big),\end{aligned} \tag{5}$$

which responds to the distance and speed difference with gains $A$ and $B_1$ like the OVM (2), and also to the CHV's speed with gain $B_n$. It uses the range policy $V$ and the speed policy $W$ to prevent the CAV from exceeding the speed limit:

$$\begin{aligned}V(D) &= \min\{\kappa(D - D_{\rm st}), v_{\max}\},\\ W(v) &= \min\{v, v_{\max}\}.\end{aligned} \tag{6}$$

## III. SAFE CONNECTED CRUISE CONTROL

In this section, we firstly revisit the theory of control barrier functions. Then, we analyze the safety of CCC (5) and propose a safety-critical CCC law based on this theory.

### A. Background on Control Barrier Functions

Consider control systems with state $x \in \mathbb{R}^n$, input $u \in \mathbb{R}^m$, and dynamics given by locally Lipschitz continuous functions $f : \mathbb{R}^n \to \mathbb{R}^n$ and $g : \mathbb{R}^n \to \mathbb{R}^{n\times m}$:

$$\dot{x} = f(x) + g(x)u. \tag{7}$$

A locally Lipschitz continuous controller $k : \mathbb{R}^n \to \mathbb{R}^m$, $u = k(x)$ leads to the closed-loop system:

$$\dot{x} = f(x) + g(x)k(x), \tag{8}$$

whose solution is $x(t)$ for initial condition $x(0) = x_0 \in \mathbb{R}^n$.

The safety of system (8) is captured by a *safe set* $\mathcal{S}$, that is given by a continuously differentiable function $h : \mathbb{R}^n \to \mathbb{R}$:

$$\mathcal{S} = \{x \in \mathbb{R}^n : h(x) \geq 0\}. \tag{9}$$

System (8) is safe w.r.t. $\mathcal{S}$ if $x_0 \in \mathcal{S} \implies x(t) \in \mathcal{S}, \forall t \geq 0$. Nagumo's theorem [19] establishes safety for (8).

**Theorem 1** ([19]). *Let $h$ satisfy $\nabla h(x) \neq 0$ for all $x \in \mathbb{R}^n$ such that $h(x) = 0$. System (8) is safe w.r.t. $\mathcal{S}$ if and only if:*

$$\dot{h}\big(x, k(x)\big) \geq 0, \quad \forall x \in \mathbb{R}^n \text{ s.t. } h(x) = 0, \tag{10}$$

*where:*

$$\dot{h}\big(x, k(x)\big) = \nabla h(x)\big(f(x) + g(x)k(x)\big). \tag{11}$$

While condition (10) describes the safety of (8) with given controller, *control barrier functions (CBFs)* [20] enable safety-critical controller synthesis for (7).

**Definition 1** ([20]). Function $h$ is a *control barrier function* for (7) on $\mathcal{S}$ if there exists $\alpha \in \mathcal{K}^{\rm e}$ such that for all $x \in \mathcal{S}$:

$$\sup_{u \in \mathbb{R}^m} \dot{h}(x, u) > -\alpha\big(h(x)\big). \tag{12}$$

Here $\alpha \in \mathcal{K}^{\rm e}$ is an extended class-$\mathcal{K}$ function. For simplicity, here we choose the linear function $\alpha(r) = \gamma r$ with $\gamma > 0$.

**Theorem 2** ([20]). *If $h$ is a CBF for (7) on $\mathcal{S}$, then any locally Lipschitz continuous controller $k$ that satisfies:*

$$\dot{h}\big(x, k(x)\big) \geq -\gamma h(x), \tag{13}$$

*for all $x \in \mathcal{S}$ renders (8) safe w.r.t. $\mathcal{S}$.*

CBFs are often used in safety filters that transform a desired but not necessarily safe controller $k_{\rm d} : \mathbb{R}^n \to \mathbb{R}^m$ into a safe controller, by using (13) in optimization:

$$\begin{aligned}k(x) = \underset{u \in \mathbb{R}^m}{\operatorname{argmin}} \quad & \|u - k_{\rm d}(x)\|^2\\ \text{s.t.} \quad & \dot{h}(x, u) \geq -\gamma h(x).\end{aligned} \tag{14}$$

If the input $u$ is scalar and $\nabla h(x) g(x) < 0$ holds, which will be the case for CCC (5), then (10) is equivalent to:

$$k_{\rm s}(x) - k(x) \geq 0, \quad \forall x \in \mathbb{R}^n \text{ s.t. } h(x) = 0, \tag{15}$$

while (14) is equivalent to [14]:

$$k(x) = \min\{k_{\rm d}(x), k_{\rm s}(x)\}, \tag{16}$$

with:

$$k_{\rm s}(x) = -\frac{\nabla h(x) f(x) + \gamma h(x)}{\nabla h(x) g(x)}. \tag{17}$$

Here, the safety filter intervention is influenced by the choice of parameter $\gamma$. Smaller $\gamma$ encourages earlier intervention.

### B. Safe Nominal CCC Design

Now we apply CBF theory to analyze the safety of system (4) with the nominal CCC (5), and to propose a provably safe CCC law. As first step, we write (4) in the form of (7) with $f(x) = [v_{i+1} - v_i \ 0]^\top$ and $g(x) = [0 \ 1]^\top$. Second, we select function $h$ to describe the safety of the CAV. Several safety criteria were proposed in [13]. Here we use the strictest criterion that requires the *time headway* $D_i/v_i$ of the CAV to be kept above a safe value $T_{\rm h} = 1/\kappa_{\rm sf}$:

$$h(x) = \kappa_{\rm sf}(D_i - D_{\rm sf}) - v_i. \tag{18}$$

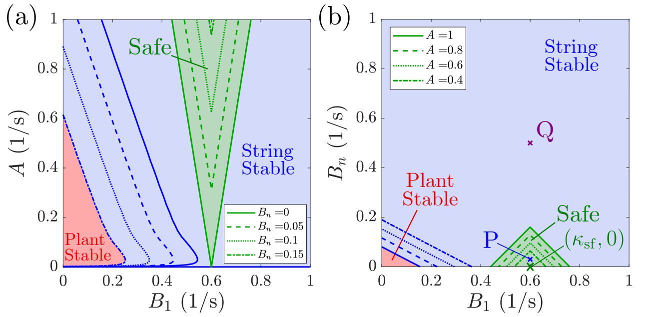


Fig. 2. Safety and stability charts of the nominal CCC (5) w.r.t. the time headway criterion (18) in (a) $(B_1, A)$ parameter space and (b) $(B_1, B_n)$ parameter space.

while including a safe standstill distance $D_{\rm sf}$. This leads to $\nabla h(x) = [\kappa_{\rm sf} \;\; -1] \neq 0$ and $\nabla h(x) g(x) = -1 < 0$, thus formulas (15) and (16) can be applied for safety analysis and safety-critical control, respectively, where $k_{\rm s}$ in (17) reads:

$$k_{\rm s}(x) = \kappa_{\rm sf}(v_{i+1} - v_i) + \gamma\big(\kappa_{\rm sf}(D_i - D_{\rm sf}) - v_i\big). \quad (19)$$

We study the safety of the nominal CCC (5) via Theorem 1, and derive the following safe choices of $(A, B_1, B_n)$ control gains by analyzing when condition (15) holds.

**Theorem 3.** *System (4) with $u_i = k_{\rm d}(x)$ given by (5) and $A, B_1, B_n \geq 0$ is safe w.r.t. $\mathcal{S}$ given by (9) and (18) if:*

- *$v_i \geq 0$, $B_1 = \kappa_{\rm sf} \geq \kappa$, $B_n = 0$ and $D_{\rm st} \geq D_{\rm sf}$; or*
- *$v_i \geq 0$, $|v_{i+1} - v_i| \leq \bar{v}$ and $|v_{i+n} - v_i| \leq \bar{v}$ with some $\bar{v} > 0$, $D_{\rm st} > D_{\rm sf}$, $\kappa_{\rm sf} \geq \kappa$ and:*

$$A \geq \frac{\big(|\kappa_{\rm sf} - B_1| + |B_n|\big)\bar{v}}{\kappa(D_{\rm st} - D_{\rm sf})}. \quad (20)$$

*Proof.* We prove safety via Theorem 1, by proving that (15) holds for $k(x) = k_{\rm d}(x)$. We consider $h(x) = \kappa_{\rm sf}(D_i - D_{\rm sf}) - v_i = 0$ and express $k_{\rm s}(x) - k_{\rm d}(x)$ by substituting (5) and (19):

$$\begin{aligned} k_{\rm s}(x) - k_{\rm d}(x) &= \kappa_{\rm sf}(v_{i+1} - v_i) - A\big(V(D_i) - v_i\big) \\ &- B_1\big(W(v_{i+1}) - v_i\big) - B_n\big(W(v_{i+n}) - v_i\big). \quad (21) \end{aligned}$$

Based on (6), we use $V(D_i) \leq \kappa(D_i - D_{\rm st})$, $W(v_i) \leq v_i$:

$$\begin{aligned} k_{\rm s}(x) - k_{\rm d}(x) &\geq \kappa_{\rm sf}(v_{i+1} - v_i) - A\big(\kappa(D_i - D_{\rm st}) - v_i\big) \\ &- B_1\big(v_{i+1} - v_i\big) - B_n\big(v_{i+n} - v_i\big). \quad (22) \end{aligned}$$

Then we add $Ah(x) = 0$ to both sides, which leads to:

$$\begin{aligned} k_{\rm s}(x) - k_{\rm d}(x) &\geq A(\kappa_{\rm sf} - \kappa)(D_i - D_{\rm sf}) + A\kappa(D_{\rm st} - D_{\rm sf}) \\ &+ (\kappa_{\rm sf} - B_1)(v_{i+1} - v_i) - B_n(v_{i+n} - v_i). \quad (23) \end{aligned}$$

Note that $v_i \geq 0$ implies $D_i - D_{\rm sf} \geq 0$ for $h(x) = 0$. Thus, the conditions in the first bullet point of Theorem 3 and (23) give (15), and it proves safety. The second bullet point yields:

$$k_{\rm s}(x) - k_{\rm d}(x) \geq A\kappa(D_{\rm st} - D_{\rm sf}) - |\kappa_{\rm sf} - B_1|\bar{v} - |B_n|\bar{v}. \quad (24)$$

Hence, (15) and safety follows for $D_{\rm st} > D_{\rm sf}$ and (20). $\square$

Fig. 2(a) and (b) visualize condition (20) in the $(B_1, A)$ space for various $B_n$ and in the $(B_1, B_n)$ space for various $A$ values, respectively, for the parameters in Table I. These plots are called *safety charts* [12], [13], where the safe domain (green) indicates safe choices of CCC parameters. In Fig. 2(a), the safe region moves towards larger $A$ values as $B_n$ increases, i.e., increased response to the CHV's speed makes it more challenging to implement provably safe gains. In Fig. 2(b), the safe region shrinks to the point $(\kappa_{\rm sf}, 0)$ as $A$ decreases. The safety charts are plotted on top of the *stability charts* from [1] for $n = 2$ in CCC (5). These charts describe both *plant stability* and *head-to-tail string stability* [1], [21]. The former means that vehicles are able to approach a constant speed in an asymptotically stable manner, and the latter indicates that speed perturbations are attenuated as they propagate from the head to the tail vehicle according to the transfer function of the linearized dynamics. For gains in the string stable domain (blue), the CAV's speed is both asymptotically stable and has smaller fluctuations than the CHV. Notice that in this case, the safe domain lies inside the string stable one.

TABLE I

PARAMETERS OF THE NUMERICAL CASE STUDIES

| Vehicle | Variable | Symbol | Value | Unit |
|---|---|---|---|---|
| All | speed limit | $v_{\max}$ | 25 | m/s |
| | standstill distance | $D_{\rm st}$ | 5 | m |
| HV | delay | $\tau$ | 1 | s |
| | range policy gradient | $\kappa_{\rm h}$ | 0.6 | 1/s |
| | driver parameters | $(A_{\rm h}, B_{\rm h})$ | $(0.1, 0.6)$ | 1/s |
| CAV | range policy gradient | $\kappa$ | 0.6 | 1/s |
| | safe gains (point P) | $(A, B_1, B_n)$ | $(0.4, 0.6, 0.03)$ | 1/s |
| | unsafe gains (point Q) | $(A, B_1, B_n)$ | $(0.4, 0.6, 0.5)$ | 1/s |
| | safe distance | $D_{\rm sf}$ | 1 | m |
| | inverse time headway | $\kappa_{\rm sf}$ | 0.6 | 1/s |
| | speed difference limit | $\bar{v}$ | 15 | m/s |
| | CBF parameter | $\gamma$ | 1 | 1/s |
| CHV | deceleration | $a_{\rm dec}$ | 7 | m/s$^2$ |
| | acceleration | $a_{\rm acc}$ | 3 | m/s$^2$ |
| | speed perturbation | $v_{\rm pert}$ | 15 | m/s |

### C. Safety-critical CCC

The safety chart in Fig. 2 helps us choose the parameters of the nominal CCC (5) in a safe way. However, compared to the string stable domain, the safe domain is small. This small set of safe parameters may lead to undesired CCC performance, i.e., low energy efficiency or high speed fluctuations, as studied below. To tackle this problem, we propose to use the *safety-critical CCC* given by (5),(16). This allows us to optimize the gains of the nominal CCC (5) to achieve the best performance, while the safety filter (16) intervenes when it is necessary to guarantee safety.

To show this, we simulate a case where the CAV responds to the CHV $n = 2$ vehicles ahead, with various controllers:

- nominal CCC (5) with safe gains (point P in Fig. 2(b)),
- nominal CCC (5) with unsafe gains (point Q),
- safety-critical CCC (5),(16) with unsafe gains (point Q).

The results are shown in Fig. 3(a)-(d) by blue, teal and orange dashed lines, respectively, for the parameters in Table I.

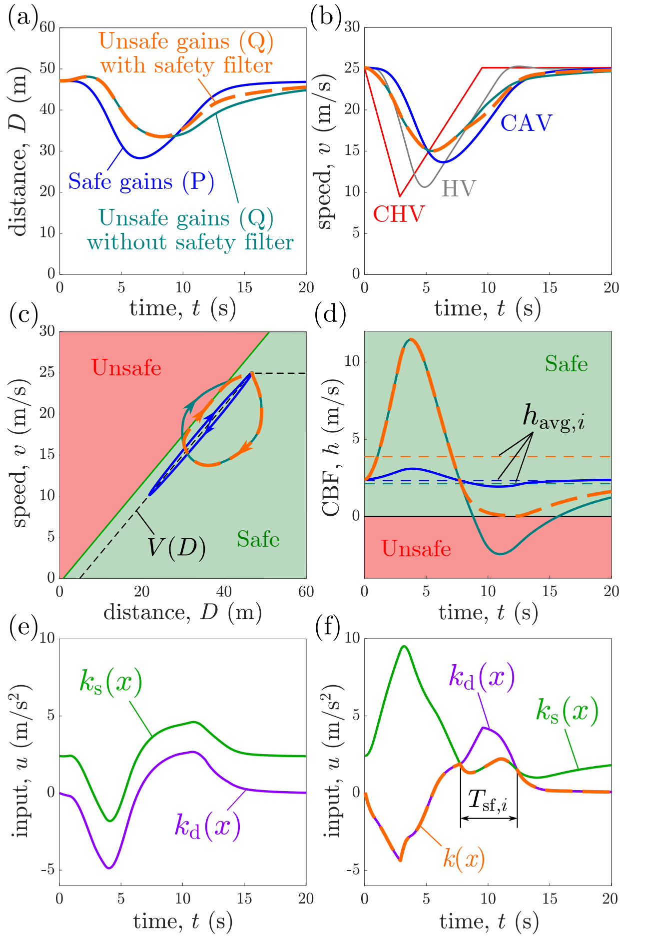


Fig. 3. (a)-(d) Simulations of system (1),(4) for $n = 2$ using the nominal CCC (5) with safe gains (blue) and unsafe gains (teal) and using the safety-critical CCC (5),(16) with a safety filter (orange). Nominal and safe control inputs using (e) safe gains, and (f) unsafe gains with safety filter.

The simulation captures a scenario where the CHV performs an emergency brake with deceleration $a_{\mathrm{dec}}$ and then returns to its original speed with acceleration $a_{\mathrm{acc}}$, leading to a speed perturbation of size $v_{\mathrm{pert}}$. As shown in Fig. 3(a)-(d), using CCC, the CAV responds to both the HV and CHV, by decelerating and then accelerating. In panels (c)-(d) we can observe the behavior expected from the safety charts in Fig. 2(b): the trajectory leaves the safe set with unsafe gains Q (teal), while it stays within the safe set with safe gains P (blue). Additionally, the safety-critical CCC (5),(16) successfully guarantees safety even with the unsafe gains (orange), as stated by Theorem 2.

Fig. 3(e)-(f) demonstrate the safety filter intervention by showing the nominal CCC input (5) and safe controller input (19), i.e., $k_{\mathrm{d}}(x)$ and $k_{\mathrm{s}}(x)$. For safe gains P in panel (e), $k_{\mathrm{d}}(x)$ is smaller than $k_{\mathrm{s}}(x)$, which means that the safety filter would not intervene. While for unsafe gains Q in panel (f), the safety filter (16) intervenes when $k_{\mathrm{d}}(x)$ exceeds $k_{\mathrm{s}}(x)$ and switches the input to $k_{\mathrm{s}}(x)$ to guarantee safety. The duration of safety filter intervention is denoted as $T_{\mathrm{sf},i}$.

Observe that the safety filter engages during acceleration rather than deceleration; see orange curves in Fig. 3(b) and (f). This is because the CAV matches its speed to the CHV. When the CHV decelerates, the CAV responds to it and brakes earlier than the HV. This increases the distance and improves safety; see Fig. 3(a). However, when the CHV accelerates after braking, the CAV starts to increase its speed while the HV still has low speed. Although this could endanger safety for the nominal CCC, the safety filter intervenes to mitigate the acceleration and keep safe distance.

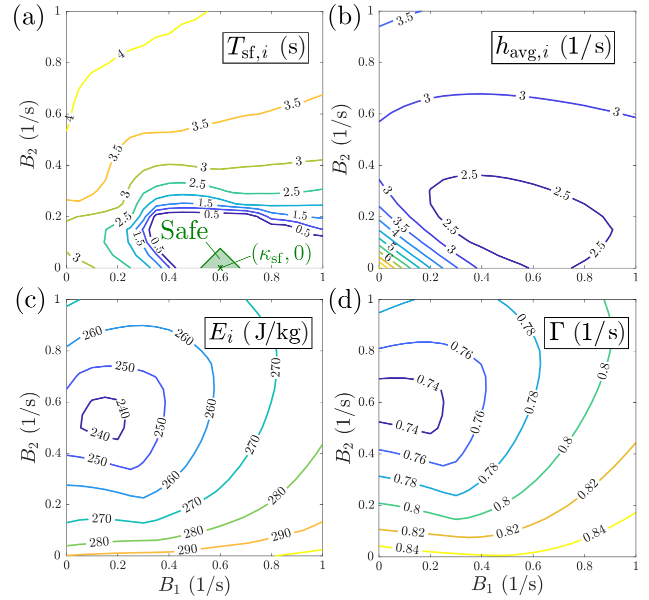


Fig. 4. Parameter dependence of safety-critical CCC (5),(16), evaluated by (a) safety filter intervention time $T_{\mathrm{sf},i}$, (b) average CBF value $h_{\mathrm{avg},i}$, (c) energy consumption per unit mass $E_i$, and (d) string stability index $\Gamma$.

To study how the gains $B_1, B_n$ affect the performance and behavior of the safety-critical CCC (5),(16), we conduct large numbers of simulations and evaluate the following metrics:

- *safety filter intervention time*, $T_{\mathrm{sf},i}$;
- *average CBF value*,

$$h_{\mathrm{avg},i} = \frac{1}{T} \int_0^T h\big(x(t)\big) \, \mathrm{d}t, \tag{25}$$

  where $T$ is the simulation time;
- *energy consumption per unit mass* [18],

$$E_i = \int_0^T v_i(t) \max\big\{0, \dot{v}_i(t)\big\} \, \mathrm{d}t; \tag{26}$$

- *string stability index* [22],

$$\Gamma = \frac{1}{N} \sum_{k=0}^{N-1} \Gamma_k, \quad \Gamma_k = \frac{\max_{t \geq 0} |v_k(t) - v_k(0)|}{\max_{t \geq 0} |v_N(t) - v_N(0)|}, \tag{27}$$

  where $N$ is the number of simulated vehicles.

The safety filter intervention time evaluates how long the CAV is in dangerous situation, while the average CBF value describes the overall safety level of the CAV during the whole simulation. For $\Gamma \leq 1$, the string stability index implies string stability (i.e., smaller velocity perturbations than those of the CHV) for the vehicle chain on average (which is different from head-to-tail string stability).

The simulation results are depicted in Fig. 4 for $n = 2$. As shown in Fig. 4(a), the CAV requires the least safety filter intervention for $B_1$ near $\kappa_{\mathrm{sf}}$ and $B_2$ near zero, which correspond to the safe region in Fig. 2(b). However, considering

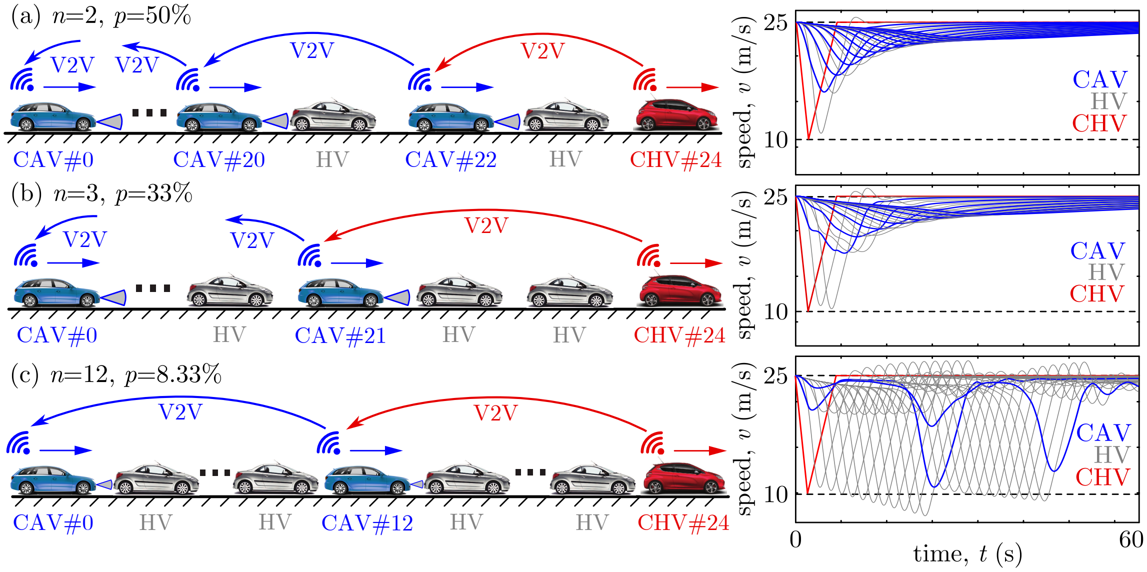


Fig. 5. Safe connected cruise control in traffic flows with different penetrations of CAVs: (a) 50%, (b) 33% and (c) 8.33%.

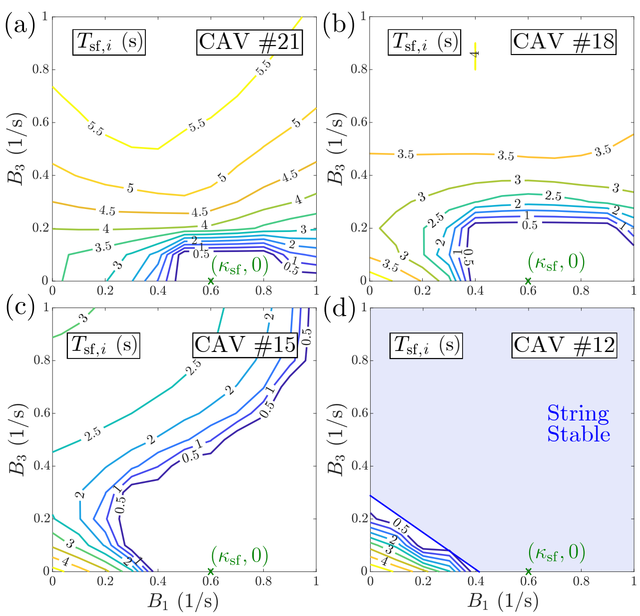


Fig. 6. Safety filter intervention time for various CAVs in the traffic flow: (a) CAV #21, (b) CAV #18, (c) CAV #15 and (d) CAV #12 in Fig. 5(b), where $n = 3$.

the overall safety during the simulation, larger $B_2$ is preferred since it leads to higher average CBF value in Fig. 4(b). This can be explained by Fig. 3(d). Compared to small $B_2$ (blue), CCC with large $B_2$ (orange) decelerates earlier and significantly increases the CBF value. Meanwhile, large $B_2$ yields small CBF value during acceleration, but the CBF value is nonnegative thanks to the safety filter. Thus, more reliance on connectivity (larger $B_2$) considerably improves the overall safety, especially during deceleration, but it also needs more safety filter intervention during acceleration.

Additionally, small $B_1$ and large $B_2$ lead to both high energy efficiency and string stability; see the similar trends in Fig. 4(c)-(d). These intuitively show the trade-off between the requirements of safety and performance. Remarkably, the proposed safety filter allows the controller to use control gains with good performance and it intervenes in dangerous situations only, as shown by the simulations.

## IV. SCALING UP SAFE CCC IN MIXED TRAFFIC

Now, we simulate mixed traffic flows with different penetrations of CAVs executing safety-critical CCC. We consider $N = 24$ follower vehicles, where every $n$th vehicle is CAV, i.e., the setup in Fig. 1(a) is concatenated $M = N/n$ times, see Fig. 5. Hence, there are $M$ CAVs with indices $i \in I = \{0, n, 2n, \ldots, (M-1)n\}$. Fig. 5 illustrates simulation results for $n = 2, 3$ and 12, with parameters in Table I. Notice that the CAVs attenuate speed fluctuations, which makes driving at the tail of the vehicle chain less dangerous.

Fig. 6 evaluates the safety filter intervention time of various CAVs for $n = 3$. Similar to Fig. 4(a), large $B_1$ (near $\kappa_{\mathrm{sf}}$) and small $B_3$ (near 0) requires minimal intervention, while large $B_3$ and small $B_1$ needs maximal intervention. As the speed perturbation reduces for the subsequent CAVs, cf. Fig. 5(b), the low-intervention region with $T_{\mathrm{sf},i} \leq 0.5$ s expands towards large $B_3$ and then to smaller $B_1$; see CAVs #18 and #15. Finally, the safety filters of CAVs at the end of the chain (#12 to #0) do not intervene for most parameter pairs, except for small $(B_1, B_3)$ that cause string instability with amplifying speed perturbations; cf. Fig. 2(b).

Another important factor affecting safety and performance is the CAV penetration. Considering the setup of Fig. 5, where every $n$th vehicle is CAV, the penetration is defined by $p = 1/n$. Next, we simulate 24 vehicles with various CAV penetrations by considering $n \in \{1, 2, 3, 4, 6, 8, 12\}$. Note that for low penetrations, HVs tend to shape the overall traffic behavior. HVs amplify speed fluctuations along the vehicle chain for our parameters; cf. Fig. 5. To avoid exceedingly large speed fluctuations and negative speeds, we reduced the CHV's speed perturbation to $v_{\mathrm{pert}} = 12$ m/s. We evaluate the average of the previous metrics for CAVs as a function of the penetration:

$$T_{\mathrm{sf,avg}} = \frac{1}{M}\sum_{i\in I} T_{\mathrm{sf},i}, \;\; H_{\mathrm{avg}} = \frac{1}{M}\sum_{i\in I} h_{\mathrm{avg},i}, \;\; E_{\mathrm{avg}} = \frac{1}{M}\sum_{i\in I} E_i. \tag{28}$$

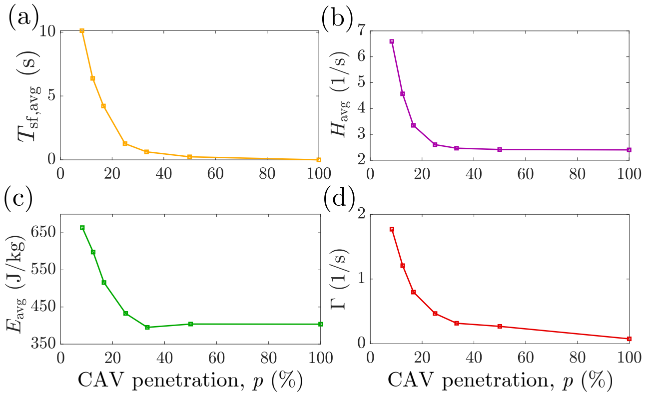


Fig. 7. Performance of safety-critical CCC (5),(16) versus CAV penetration: (a) average safety filter intervention time $T_{\rm sf,avg}$, (b) average CBF value $H_{\rm avg}$, (c) average energy consumption per unit mass $E_{\rm avg}$, (d) string stability index $\Gamma$.

Fig. 7 shows the simulation results for a pair of $(B_1, B_n)$ gains (point Q). Fig. 7(a) displays that the safety filter intervention drops significantly with increasing penetration from 0 to 30%. Above 30%, the decline is less pronounced. The average CBF value in Fig. 7(b) also decreases with the penetration. These are explained similar to Fig. 3(d): as the penetration decreases, CAVs match their speed with connected vehicles farther ahead, which makes them brake earlier and increase the CBF significantly during deceleration, while it yields more safety filter intervention during acceleration. Similar trends are observed for energy consumption and string stability in Fig. 7(c)-(d). Energy efficiency improves considerably between 0% and 30% penetration and reaches the minimum at 33% ($n = 3$) for our gains. String stability ($\Gamma \leq 1$) requires at least 16.7% penetration ($n \leq 6$).

Overall, for low CAV penetration, a slight increase of penetration level significantly improves safety and performance. CAV penetrations around 15-20% already yield small safety filter intervention and high performance, while larger penetrations may not lead to considerable improvement for our setup. Importantly, the proposed safety-critical CCC (5),(16) provides safe CAV behavior in all cases.

## V. CONCLUSIONS

In this paper, we used control barrier functions to investigate the safety of connected cruise control (CCC), where connected automated vehicles (CAVs) respond to multiple vehicles ahead of them. Particularly, we derived safe CCC parameter choices via safety charts, and we proposed *safety-critical CCC* to maintain safety while achieving high performance. We highlighted by simulations that connectivity to vehicles farther ahead improves the safety of CAVs during deceleration, but it requires safety filter intervention during acceleration. Additionally, increasing the penetration of CAVs in mixed traffic improves safety, energy efficiency and string stability. As future research, we plan to take the system delay into account in safety-critical CCC.

## REFERENCES


[1] L. Zhang and G. Orosz, "Motif-based design for connected vehicle systems in presence of heterogeneous connectivity structures and time delays," *IEEE Transactions on Intelligent Transportation Systems*, vol. 17, no. 6, pp. 1638–1651, 2016.

[2] A. Vahidi and A. Sciarretta, "Energy saving potentials of connected and automated vehicles," *Transportation Research Part C*, vol. 95, pp. 822–843, 2018.

[3] S. Cui, B. Seibold, R. Stern, and D. B. Work, "Stabilizing traffic flow via a single autonomous vehicle: Possibilities and limitations," in *IEEE Intelligent Vehicles Symposium*, 2017, pp. 1336–1341.

[4] Y. Zheng, J. Wang, and K. Li, "Smoothing traffic flow via control of autonomous vehicles," *IEEE Internet of Things Journal*, vol. 7, no. 5, pp. 3882–3896, 2020.

[5] A. Alam, A. Gattami, K. H. Johansson, and C. J. Tomlin, "Guaranteeing safety for heavy duty vehicle platooning: Safe set computations and experimental evaluations," *Control Engineering Practice*, vol. 24, pp. 33–41, 2014.

[6] P. Nilsson, O. Hussien, A. Balkan, Y. Chen, A. D. Ames, J. W. Grizzle, N. Ozay, H. Peng, and P. Tabuada, "Correct-by-construction adaptive cruise control: Two approaches," *IEEE Transactions on Control Systems Technology*, vol. 24, no. 4, pp. 1294–1307, 2015.

[7] C. Massera Filho, M. H. Terra, and D. F. Wolf, "Safe optimization of highway traffic with robust model predictive control-based cooperative adaptive cruise control," *IEEE Transactions on Intelligent Transportation Systems*, vol. 18, no. 11, pp. 3193–3203, 2017.

[8] A. Ames, J. Grizzle, and P. Tabuada, "Control barrier function based quadratic programs with application to adaptive cruise control," in *53rd IEEE Conference on Decision and Control*, 2014, pp. 6271–6278.

[9] F. Hu and H. Yu, "Safety-critical lane-change control for CAV platoons in mixed autonomy traffic using control barrier functions," *arXiv preprint*, no. arXiv:2302.00424, 2023.

[10] C. Zhao, H. Yu, and T. G. Molnar, "Safety-critical traffic control by connected automated vehicles," *Transportation Research Part C*, vol. 154, p. 104230, 2023.

[11] G. Gunter, M. Nice, M. Bunting, J. Sprinkle, and D. B. Work, "Experimental testing of a control barrier function on an automated vehicle in live multi-lane traffic," in *Workshop on Data-Driven and Intelligent Cyber-Physical Systems for Smart Cities*, 2022, pp. 31–35.

[12] C. R. He and G. Orosz, "Safety guaranteed connected cruise control," in *21st IEEE International Conference on Intelligent Transportation Systems*, 2018, pp. 549–554.

[13] T. G. Molnar, G. Orosz, and A. D. Ames, "On the safety of connected cruise control: Analysis and synthesis with control barrier functions," in *62nd IEEE Conference on Decision and Control (CDC)*, 2023, pp. 1106–1111.

[14] A. Alan, A. J. Taylor, C. R. He, A. D. Ames, and G. Orosz, "Control barrier functions and input-to-state safety with application to automated vehicles," *IEEE Transactions on Control Systems Technology*, vol. 31, no. 6, pp. 2744–2759, 2023.

[15] M. Bando, K. Hasebe, K. Nakanishi, and A. Nakayama, "Analysis of optimal velocity model with explicit delay," *Physical Review E*, vol. 58, no. 5, p. 5429, 1998.

[16] T. G. Molnar, A. K. Kiss, A. D. Ames, and G. Orosz, "Safety-critical control with input delay in dynamic environment," *IEEE Transactions on Control Systems Technology*, vol. 31, no. 4, pp. 1507–1520, 2023.

[17] W. Xiao, C. A. Belta, and C. G. Cassandras, "Sufficient conditions for feasibility of optimal control problems using control barrier functions," *Automatica*, vol. 135, p. 109960, 2022.

[18] J. I. Ge, S. S. Avedisov, C. R. He, W. B. Qin, M. Sadeghpour, and G. Orosz, "Experimental validation of connected automated vehicle design among human-driven vehicles," *Transportation Research Part C: Emerging Technologies*, vol. 91, pp. 335–352, 2018.

[19] M. Nagumo, "Über die lage der integralkurven gewöhnlicher differentialgleichungen," *Proceedings of the Physico-Mathematical Society of Japan. 3rd Series*, vol. 24, pp. 551–559, 1942.

[20] A. D. Ames, X. Xu, J. W. Grizzle, and P. Tabuada, "Control barrier function based quadratic programs for safety critical systems," *IEEE Transactions on Automatic Control*, vol. 62, no. 8, pp. 3861–3876, 2017.

[21] D. Liu, B. Besselink, S. Baldi, W. Yu, and H. L. Trentelman, "On structural and safety properties of head-to-tail string stability in mixed platoons," *IEEE Transactions on Intelligent Transportation Systems*, vol. 24, no. 6, pp. 6614–6626, 2023.

[22] S. Guo, G. Orosz, and T. G. Molnar, "Connected cruise and traffic control for pairs of connected automated vehicles," *IEEE Transactions on Intelligent Transportation Systems*, vol. 24, no. 11, pp. 12 648–12 658, 2023.